MAXI Catalog: Source Detection and Sensitivity

Kazuo Hiroi[1], Yoshihiro Ueda[1], Satoshi Eguchi[1], and the MAXI team

[1]Department of Astronomy, Kyoto University, Kyoto 606-8502, Japan
E-mail (K.H.): hiroi@kusastro.kyoto-u.ac.jp

Abstract

The MAXI source catalog will become a unique database of X-ray populations covering the 0.5–30 keV band in all sky. It will contain more than 1,300 AGNs (Ueda et al. 2008), including many new sources. We develop a software program of source detection of faint sources from MAXI/GSC data, where maximum likelihood fit is performed to a projected image by taking into account the image response and background. In this paper, we present our study to estimate the realistic sensitivities and the position accuracy of MAXI based on simulations.

Key words: catalogs — galaxies:active — X-rays:galaxies — X-rays:general

1. INTRODUCTION

One of the main goals of the MAXI mission is to provide a new X-ray catalog from the entire sky, including both transient and persistent sources. The Gas Slit Cameras (GSCs; Mihara et al. 2008) and the Solid-state Slit Cameras (SSCs; Tomida et al. 2008) cover the energy band of 2–30 keV and 0.5–12 keV, respectively, with unprecedented sensitivities as an all-sky mission. In particular, the large effective area of the GSCs at energies above 2 keV enables us to detect absorbed Active Galactic Nuclei (AGNs) that were missed in the ROSAT All Sky Survey, thus providing a unique database of extragalactic populations.

In this paper, we quantitatively evaluate the sensitivity and position accuracy of the MAXI GSCs, which are the most fundamental properties of the source catalog. Here we extensively utilize the MAXI simulator developed by Eguchi et al. (2008).

2. ANALYSIS METHOD

2.1. Simulation

We first produce simulated data of MAXI, to which our source detection method described in the next subsection is applied. In this paper, we only treat an extragalactic point-like source over the cosmic X-ray background, with two different operation times, 1 week and 1 orbit (90 minutes) as representative cases. In the 1 week simulation, we assume as real conditions as possible, by adopting realistic orbit and attitude information of MAXI and avoiding sky region around the Sun and the epoch of the South Atlantic Anomaly (SAA) passage. All the twelve GSCs are turned on, and their photons are summed in the image analysis. In the case of the 1 orbit simulation (i.e., only one exposure by a single camera for a given target), we assume three different directions of incident photons into the MAXI cameras as illustrated in Figure 1. The Sun and SAA are ignored. We only use data of the six GSCs with the zenithal field-of-view in the analysis to simulate the detection of very short-lived (< 20 minutes) transients. The simulation conditions are summarized below.

- Software
  - maxisim ver.6.3.102 (simulation)
  - dis45 ver.2.04 (image analysis)
- Source Spectrum
  - Crab-like (a power law of $\Gamma = 2.1$)
- Non X-ray Background Rate
  - 10 counts/s/counter
- Energy Band Used in the Analysis
  - 2–30 keV
- Exposure (Operation Time)
  - 1 week, or 1 orbit

2.2. Image Fit

To extract the best sensitivities from the data, we have developed an analysis method by employing image fitting with the maximum likelihood algorithm. Firstly, we project the positions in RA and DEC of photon events around the target in the "sky coordinates", similar to image analysis of pointing satellites. To derive the flux, the position and their errors of the target, we perform 2-dimensional fitting to this simulated image by a model consisting of the point spread function (PSF) and background (the non X-ray background and the cosmic X-ray background).

One complexity in the analysis of MAXI data is that the PSF and background are position dependent, being determined by the orbit and attitude condition. To take this into account, we also utilize the MAXI simulator to construct the PSF and background models with a sufficiently larger number of photons to suppress the statistical fluctuation. An example of the PSF model integrated for the 1-week observation is shown in Figure 2.

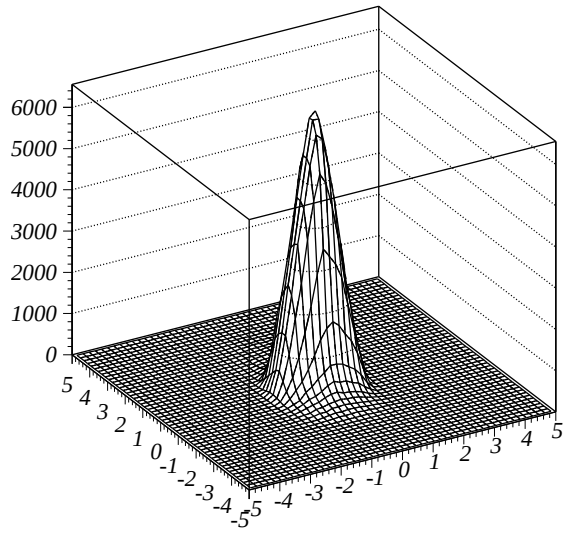

Fig. 2. An example of the PSF in the sky coordinate in units of degree, integrated for the 1-week observation. The z-axis is arbitrary.

To properly treat statistics with small numbers of photons in each bin, we adopt the Poisson maximum likelihood algorithm, utilizing the MINUIT package. The normalization of the PSF (i.e., flux) and background level are set to be free parameters. In the image fitting process, we consider two different situations, when the position of the source is (i) unknown and (ii) known. In the former case, we also make the position of the source free. Here we assume that the shape of the PSF does not largely differ in the region of interest, and ignore its position dependence for simplicity. In the latter case, the position is fixed at the input location.

We define the detection significance (σ_D) as

$$\sigma_D = \text{(best-fit flux) / (its } 1\sigma \text{ statistical error)}$$

and set $\sigma_D \geq 5$ as the criteria for secure detection (i.e., relative $\leq$20% error in the obtained flux). To evaluate the position accuracy, we make the error contour at 90% confidence level, or more simply, calculate the root sum square of the position errors in the two (x and y) directions.

Figure 3 shows the raw (left) and smoothed (right) images around the target, located in the center, for the 1-week simulation. Figure 4 shows its projection onto X-axis in a central region (with error bars), superposed with the best-fit model (dashed line: total, dotted line: only background). The left and right figures correspond to that of the 1-week simulation and of the 1-orbit simulation, respectively. By repeating such simulations with different input fluxes, we accurately estimate the 5 σ sensitivity (see Figure 5) and the position error for a given exposure.

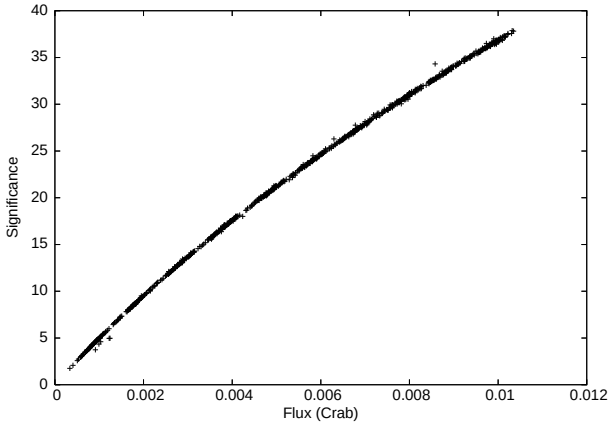

Fig. 5. The correlation between the detection significance and source flux for a 1-week simulation. The 5σ detection sensitivity is derived from this relation.

3. RESULTS

3.1. Sensitivity

The results are summarized in Table 1. In whichever case the position of the target is known or not, the 5σ sensitivity from the 1-week observation is found to be 1.0 mCrab, about 10 times better than that of the all sky monitor on RXTE. We confirm that the observing condition of this target in terms of effective exposure (i.e., exposure multiplied by the slit area) is close to the average over the entire sky. Hence, these results can be regarded as typical performance expected from MAXI. As for the result of 1-orbit simulation, we find the detection sensitivity becomes slightly ($< 10\%$) worse when the source position is unknown. It is also seen that the best sensitivity is obtained in pattern 3, where the photons from the target are collected by 2/3 of the six cameras at moderate incident angles.

Table 1. The sensitivity of MAXI/GSCs. (unit mCrab)

	position	
exposure	known	unknown
1 week	1.00	1.02
1 orbit (pattern 1)	21	23
1 orbit (pattern 2)	23	25
1 orbit (pattern 3)	20	22

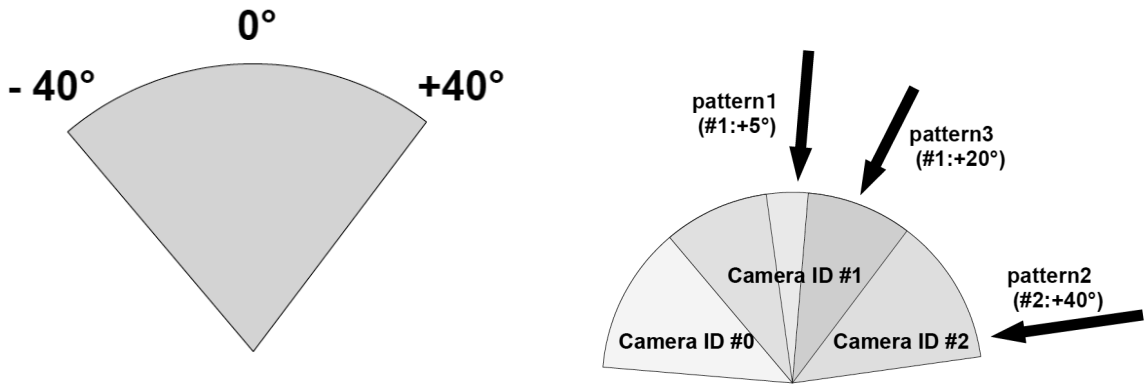

Fig. 1. The left figure shows the field of view covered by one GSC. In the simulation, we consider three patterns of incident direction of photons from a target, as illustrated in the right figure. For example, "pattern1(#1:+5°)" means that the target is located +5° away from the field-of-view center of Camera ID #1.

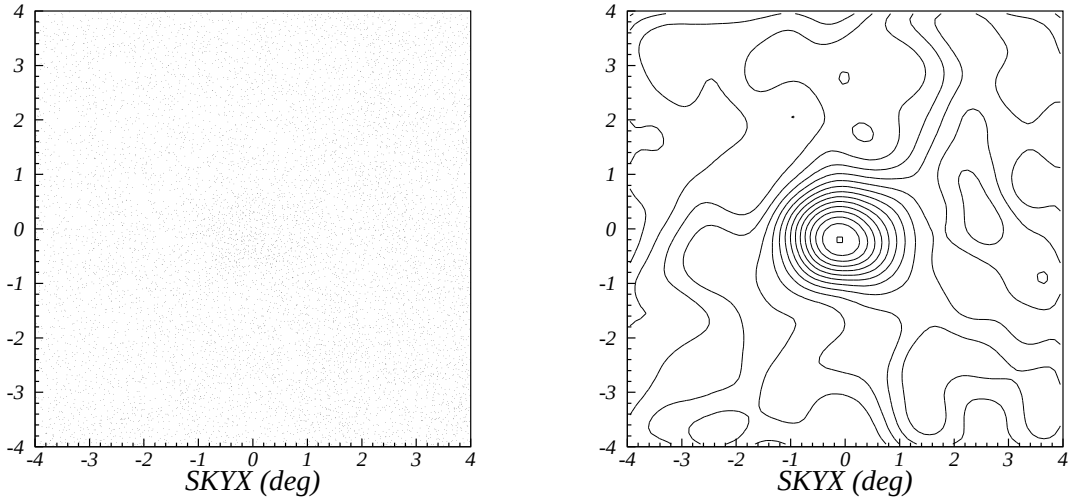

Fig. 3. An example of a simulated image around the target from a 1-week observation (left: raw, right: smoothed).The image size is 8 deg × 8 deg.

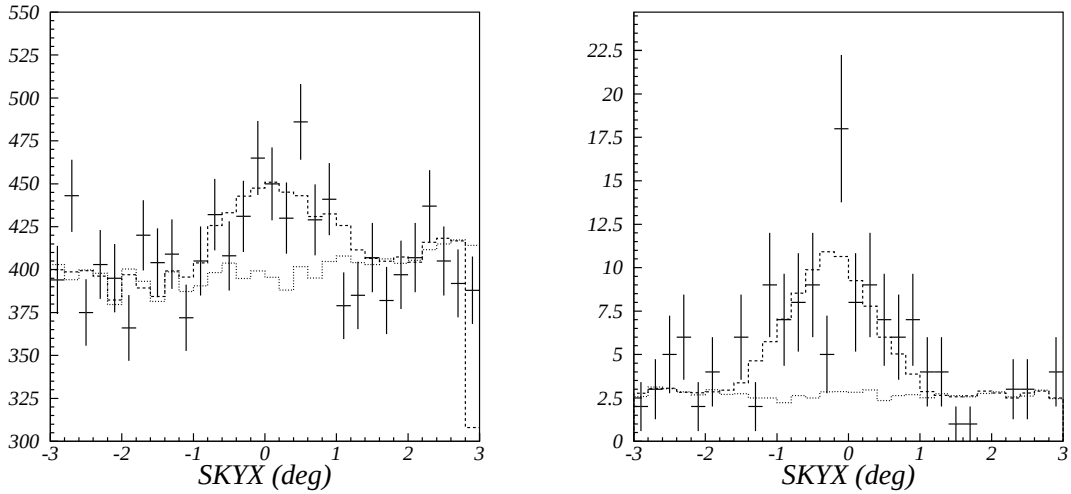

Fig. 4. The comparison of the (simulated) data and the best-fit model (left: 1 week, right: 1 orbit). The unit of vertical axis is counts per bin. We find that the background is dominant in 1-week simulation and that the source is dominant in 1-orbit one.

3.2. Position Accuracy

Figure 6 shows examples of the error contour of the detected position at 90 % confidence level. We find that a typical error radius for targets with fluxes close to the 5σ sensitivity limit is ≈0.2–0.3 degree. The relation between the flux F and the error radius (combined from the two directions) is plotted in Figure 7. We find the positional error is roughly proportional to $F^{-0.89}$, steeper than a naive expectation of $F^{-0.5}$. We infer that this is due to coupling between the position and flux determination in the fitting process.

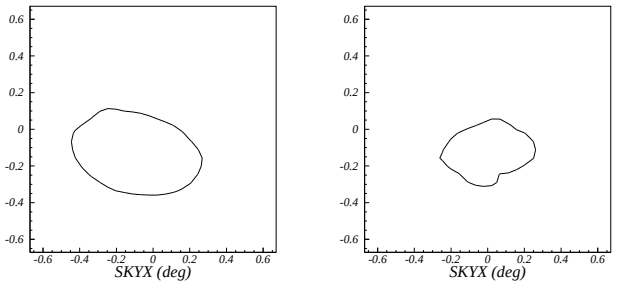

Fig. 6. Examples of the error contour of source position at 90% confidence level (left: 1 week, right: 1 orbit). The detection significance of both sources are about 5σ.

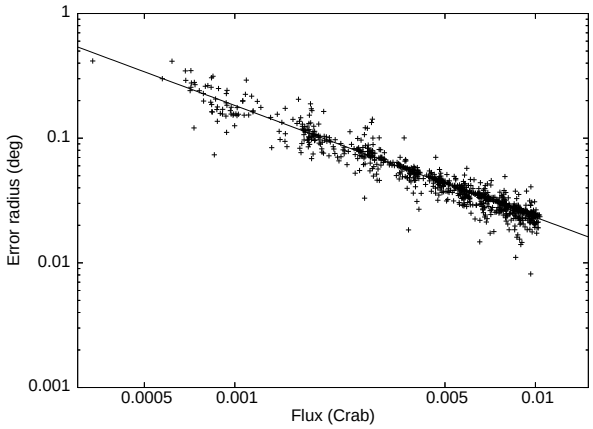

Fig. 7. The correlation between the flux and error radius (combined from the two directions). The curve shows the best-fit power law with a slope of –0.89.

4. SUMMARY

Our study shows that, by utilizing the image fitting method, we can achieve a sensitivity of about 1 mCrab for a point-like source from a 1-week operation of MAXI with typical observing conditions, assuming the non X-ray background rate of 10 c/s/counter. Based on our results, we plot a theoretical sensitivity curve as a function of operation time t in Figure 8. The sensitivity is roughly proportional to t^{-1} below $\sim 10^4$ sec (source-dominant case) but to $t^{-1/2}$ above it (background-dominant case).

This performance of MAXI is quite promising for scientific studies of not only Galactic but also extragalactic objects. We estimate that the sensitivity reaches the confusion limit (˜0.2 mCrab) from about half year operation of MAXI. At this flux level, about 1,300 AGNs are expected to be detected at Galactic latitudes larger than 15 degree. The MAXI catalog will contain many new transient and/or absorbed AGNs, and hence become a unique database of extragalactic populations complementary to other catalogs of all-sky missions, such as ROSAT, Swift/BAT, and INTEGRAL.

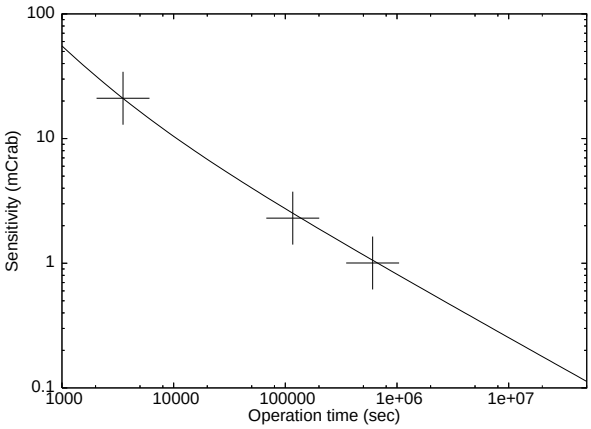

Fig. 8. Sensitivity curve as a function of integration time (actual operation time of MAXI with typical observing conditions) for a point-like source with a Crab-like spectrum. The three points correspond to the sensitivities of 1-orbit, 1-day, and 1-week observations, from left to right, obtained from our simulations.

References

Eguchi, S., et al. 2008, in this proceedings
Mihara, T., et al. 2008, in this proceedings
Tomida, H., et al. 2008, in this proceedings
Ueda, Y., et al. 2008, in this proceedings